Available online at www.sciencedirect.com

SCIENCE DIRECT®

Polymer 44 (2003) 4981–4992

polymer

www.elsevier.com/locate/polymer

Phase behavior and morphology of poly(phenylene ether)/epoxy blends

Glen D. Merfeld[a,*], Gary W. Yeager[a], Herbert S. Chao[b], Navjot Singh[c]

[a]*General Electric Global Research, Polymer and Specialty Chemical Technologies, One Research Circle, Niskayuna, NY 12309, USA*
[b]*Sartomer Company, 502 Thomas Jones Way, Exton, PA 19341, USA*
[c]*McKinsey and Company, Inc., 55 East 52nd Street, New York, NY 10055, USA*

Received 30 December 2002; received in revised form 5 May 2003; accepted 12 May 2003

Abstract

The miscibility of diglycidyl ether of bisphenol-A (DGEBA) based epoxies with a series of poly(2,6-dimethyl-1,4-phenylene ether) (PPE) resins was measured and the effects of PPE molecular weight, end-capped or grafted functionality, and blend composition were explored. Interpretation of phase behavior was aided by the use of the Flory–Huggins theory. Miscibility behavior in the unreacted blends was found to correlate with trends in phase separation during the curing reaction. The cured morphologies of these blend systems were also studied. The compatibilization effect of PPE-epoxy copolymer formation was found to play a dominant role in determining the final size of the dispersed phase, while temperature control of reaction and mass transfer kinetics were identified as a possible means of further affecting the cured morphology.

Keywords: Poly(2,6-dimethyl-1,4-phenylene ether); DGEBA epoxy; Phase behavior

1. Introduction

A thermoset can be toughened by a dispersed rubber of thermoplastic phase [1]. Dispersed thermoplastics can also confer improvements in other properties including mold shrinkage (for which they are termed low profile additives), heat performance, and electrical properties. Typically, such blends are miscible prior to reaction and then phase separate during the curing reaction to give a uniformly dispersed minor phase. Many of the enhancements in material properties are derived from or correlated with these morphological characteristics. A significant amount of work is reported in the literature on epoxy systems, predominantly for diglycidyl ether of bisphenol-A (DGEBA) type epoxies. Various thermoplastics including poly(ether sulfone) [2,3], poly(methyl methacrylate) [4], poly(caprolactone) [5], and poly(phenylene ether) [6–10] have been blended with DGEBA resins. Additionally, similar strategies have been applied to other thermoset matrices such an unsaturated polyester resins [11,12] and phenolics [13]. Several studies have probed the relationship between material characteristics and property enhancements including mechanisms of toughening [7] and models of phase separation and morphology development [14,15]. More recent developments have demonstrated the value of new thermal characterization techniques for the real-time monitoring of reaction induced phase separation and the simultaneous assessment of kinetics of phase separation and cure [3].

In this work, DGEBA blends with poly(2,6-dimethly1,-4-phenylene ether) (PPE) resins are studied further to determine how PPE molecular weight, chemical functionality, and composition of the blend influence miscibility before reaction. The Flory–Higgins theory of polymer mixtures is used to model measurements of phase behavior and to extract estimates for the interaction energy between PPE and epoxy molecules. This understanding of miscibility in the unreacted systems is then translated to phase separation during reaction and combined with gelation measurements to interpret morphology development during cure.

2. Experimental

The PPE resins used in this work are summarized in Table 1. A broad range of polymer molecular weights and

---

[*] Corresponding author. Tel.: +1-518-387-6810; fax: +1-518-387-5812. *E-mail address:* merfeld@crd.ge.com (G.D. Merfeld).

0032-3861/03/$ - see front matter © 2003 Elsevier Science Ltd. All rights reserved.
doi:10.1016/S0032-3861(03)00443-9

Table 1
PPE resins used in this study

PPE	IV (dl/g)	M_w	M_n	T_g (°C)	Functionality
PPE.09	0.09	5540	2340	144	–
PPE.12	0.12	7850	1530	164	–
PPE.15	0.15	10,960	2060	174	–
PPE.25	0.25	23,870	10,880	201	–
PPE.30	0.3	34,760	15,200	207	–
PPE.15FA4	0.15[a]	11,550	3000	173	4% FA
PPE.15FA8	0.15[a]	11,500	3120	175	8% FA
PPE.12MC	0.12[a]	8700	3390	166	Methyl capped

[a] IV measured before acid grafting or methyl capping.

three chemically modified PPE variants were investigated. Molecular weights were measured using a waters gel permeation chromatograph (GPC) with a bank of Phenomenex Phenogel 10^5, 10^4, and 500 Å columns. Polymer solutions (100 μl, approximately 0.3% by weight in chloroform) were injected and carried through the columns at a flow rate of 1.5 ml/min. Elution was monitored using a UV detector set at 254 nm. The columns were calibrated using polystyrene standards (2,000 to 860,000 g/mol). Molecular dimensions were also characterized in terms of intrinsic viscosity (IV) measurements made in chloroform at 25 °C using an Ubbelohde viscometer. Glass transition temperatures were evaluated by DSC (Perkin Elmer DSC-7) at a scan rate of 20 °C/min with onset temperature being reported. A detailed description of the PPE syntheses and microstructure characterization has been reported elsewhere [8].

Two acid-grafted PPE resins were prepared by reactive extrusion of the 0.15 IV PPE with either 4 or 8 weight percent fumaric acid (FA) in a twin screw extruder at 230 °C. Titration with a 0.1 M solution of tetrabutylammonium hydroxide in methanol was used to estimate the acid functionality at 0.45 and 0.97 mequiv. of acid per gram for the 4 and 8 percent FA-grafted PPE, respectively. Reactive extrusion had a negligible effect on the weight average molecular weight and caused only a small increase in number average molecular weight as measured by GPC. Reaction of 0.12 IV PPE with methyl iodide and sodium carbonate in toluene at 80 °C for 48 h was used to cap PPE hydroxyl end groups; ^{1}H-NMR analysis (performed on a GE QE-300 MHz NMR spectrometer) indicates nearly complete conversion of the OH groups to the OCH_3 residue. The weight averaged molecular weight measured by GPC was nominally unchanged.

Two DGEBA epoxies with the chemical structures shown in Fig. 1 were purchased under the trade names of Epon®825 and Epon®828 from the Shell Chemical Company[1]. These have respective molecular weights of approximately 355 and 374 g/mol. Blends were formulated by dissolving PPE into the epoxy at temperatures 50 to 75 °C above the PPE glass transition temperatures (T_g) listed in Table 1. For curing experiments, the homogeneous mixtures were then cooled to 150 °C before addition of 4,4-methylene bis(2,6-diethyl aniline) curing agent (Lonzacure® MDEA)[2]. The MDEA content was adjusted in blend formulations to maintain a constant amine to epoxy functionality ratio of 1:1. For each primary amine a reactive functionality of two assumed.

Blend phase separation was monitored by transmitted light intensity using a device, illustrated in Fig. 2(a), consisting of a microscope with a collimated light source, a temperature programmable sample stage, and a photoresistor. Samples for light transmission studies were prepared by placing a drop of the blend into the well of a polished microscope slide and covering with a second slide. Measurements of phase separation induced by either a temperature change (in blends not containing the curing agent) or by reaction (in blends during isothermal cure) were made. The cloud point was recorded as the temperature or time at which the transmitted light intensity began to decrease from its baseline value. For temperature ramp/quench studies, scan rates of 1 to 5 °C/min were used. An example of a temperature quench experiment is shown in Fig. 2(b) for an 80/20 blend of Epon828 and 0.12 IV PPE-this samples shows an upper critical solution temperature (UCST) of approximately 100 °C.

Gel points during cure were measured using a Sunshine® gel time meter (model 22A) in accordance with ASTM standard D3056-85[3]. For testing, reaction mixtures were transferred to Pyrex test tubes (16 × 150 mm) that were then place in a stirred oil bath maintained at temperature using an electronic controller. An increase in solution viscosity upon gelation was measured as an increase in the torsion force exerted on a slowly rotating spindle suspended in the test sample. Reproducible measurements were obtained by minimizing sample transfer time and maintaining uniform sample and spindle immersion levels. In limited studies, isothermal DSC experiments were also used to test reaction kinetics with follow-up scans to assess residual heat of reaction.

To prepare samples for morphology studies, reaction mixtures were poured into shallow aluminum pans and cured under vacuum in two stages: first at 150, 175, or 200 °C for 1 h, and then at 250 °C for 2 h. The cured samples were microtomed at room temperature to a thickness of approximately 0.1 μm, and the sections exposed to RuO_4 vapor for 20 s to preferentially stain the PPE-rich phase. A Philips 100CX TEM was used to study the samples. Image analysis of the micrographs was performed using ImagePro® software to characterize the size of dispersed domains; 70 and 130 particles were analyzed per sample[4].

---

[1] Epon® is a registered trademark of the Shell Chemical Company.

[2] Lonzacure® is registered trademark of the Lonza Corporation.

[3] Sunshine® is registered trademark of the Sunshine Instruments Company.

[4] ImagePro® is a registered trademark of Image Processing Solutions, Inc.

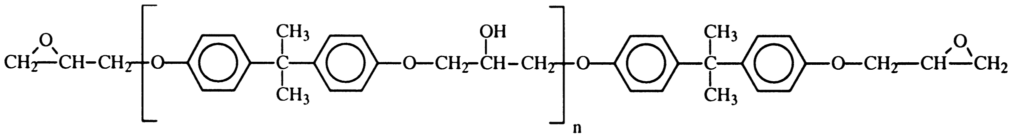

Fig. 1. Diglycidyl either of bisphenol-A (DGEBA) resin structures: Epon825, $n = 0$; Epon828, $n = 1.1$.

3. Results and discussion

3.1. Miscibility of PPE with DGEBA resins

Phase separation upon cooling, corresponding to a UCST was observed in blends of PPE and Epon828. Fig. 3 summarizes the light scattering measured phase behavior in blends with PPE resins ranging in IV from 0.09 to 0.30 dl/g. An estimated standard deviation of 1 °C was made for these measurements by studying 10 replicate blends. Some additional uncertainty may be expected at low PPE loadings where contrast between the phases in diminished. In all blends investigated, the phase separation was completely reversible such that raising the temperature above the measured UCST caused rehomogenization of the mixture. This verifies the existence of the thermodynamic phase boundary. Furthermore, the measurements were reproducible even after multiple heating and cooling cycles suggesting minimal degradation during preparation and testing, and little reaction of the PPE and epoxy in the absence of a curing additive.

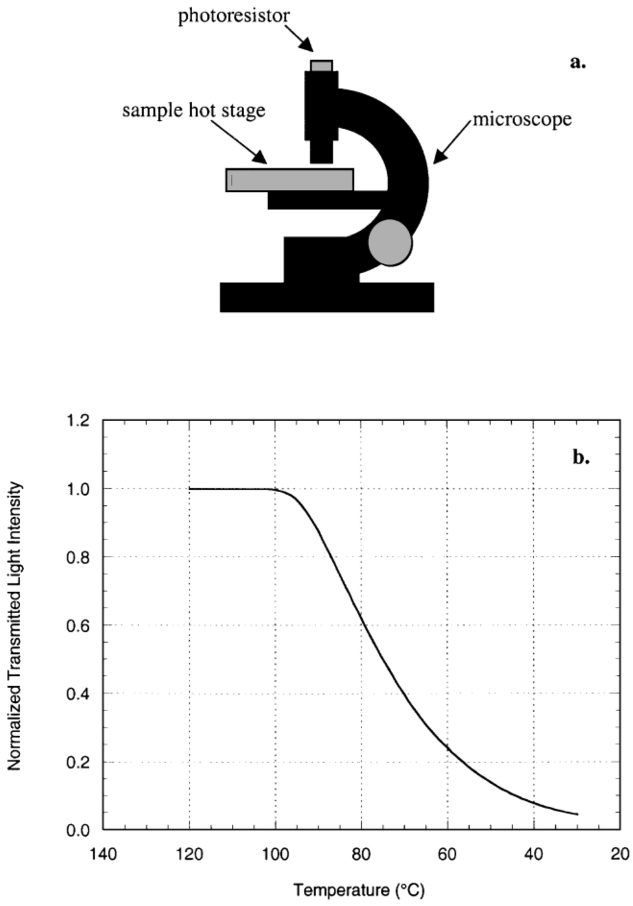

Fig. 2. (a) Illustration of apparatus used to monitor phase separation in Epoxy/PPE blends as a function of temperature or as a function of reaction time during cure. (b) Example of decrease in light intensity measured for an 80/20 Epon828/0.12 IV PPE blend upon temperature induced phase separation.

In general, a trend of increasing miscibility with lowering PPE molecular weight (or IV) is shown in Fig. 3. This response is predicted by the classic Flory–Huggins theory for polymer mixtures [16,17]

$$\Delta g_{\mathrm{mix}} = \phi_{\mathrm{A}}\phi_{\mathrm{B}}B_{\mathrm{AB}} + RT\left[\frac{\rho_{\mathrm{A}}\phi_{\mathrm{A}}\ln\phi_{\mathrm{A}}}{M_{\mathrm{A}}} + \frac{\rho_{\mathrm{B}}\phi_{\mathrm{B}}\ln\phi_{\mathrm{B}}}{M_{\mathrm{B}}}\right] \tag{1}$$

where the free energy of mixing per unit volume, Δg_{mix}, is described in terms of the volume fractions, ϕ, of components A and B in the blend and their respective densities, ρ, and molecular weights, M. For polydisperse polymers it is appropriate to use weight average molecular weights [18,19]. Mixing energetics are captured by the excess free energy term, B_{AB}, which can be described as an interaction energy density with units of energy per unit volume. This parameter is analogous to the unitless χ type interaction but has the advantage of not requiring the arbitrary and sometime ambiguous assignment of a reference volume. The bracketed terms in Eq. (1) estimate the increase in entropy derived from the combinatorial

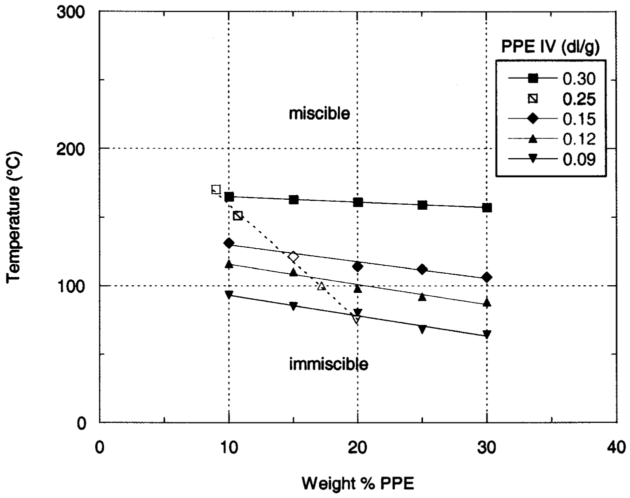

Fig. 3. Light transmission measure upper critical solution temperatures for blends of Epon828 with PPE resins of varying molecular weight; the solid line curves are included to identify trends in the data only. Critical composition blends are shown as open symbols which correspond to the PPE IV with the same filled symbol. Note, because of limited supply of 0.25 IV PPE, only its critical composition was studied. The dashed line highlights the shift in the critical composition with changing PPE molecular weight.

mixing of molecules. Inspection shows that lowering molecular weight increases the entropic component of mixing and favour miscibility. This is observed experimentally in Fig. 3.

The Flory–Huggins theory can be used to predict UCST binodal and spinodal phase boundaries when the interaction energy is known, or conversely, to extract estimates for B_{AB} from phase behavior data. The latter analysis is simplified mathematically and experimentally by considering the special case of the critical point where the third derivative of Eq. (1) with respect to composition is equal to zero. Under this condition the interaction parameter is defined as

$$B_{\text{critical}} = \frac{RT}{2}\left[\sqrt{\frac{\rho_A}{M_A}} + \sqrt{\frac{\rho_B}{M_B}}\right]^2 \tag{2}$$

and the critical composition can be calculated using

$$\phi_A = 1/[1 + (\rho_B M_A/\rho_A M_B)] \tag{3}$$

Moreover, the critical condition corresponds to the point where spinodal and binodal phase boundaries overlap. Experimental evaluation of phase behavior at the critical composition helps to avoid kinetic effects that can obscure interpretation of the binodal phase boundary. Even so, it should be recognized that in blends of highly polydisperse polymers many phase boundaries might exist and complicate interpretation of phase behavior. This can have the effect of broadening the observed cloud point and shifting the phase boundary maximum away from the critical composition. Advanced theories have been developed in attempt to address these effects and a review of these can be found in the literature [20]. Nevertheless, polydispersity effects should not severely compromise the capability of the Flory–Higgins model and its use here to aid interpretation of phase behavior observations.

By using Eq. (3) and the weight average molecular weights given in Table 1, the critical compositions for blends of the DGEBA epoxies with various PPE resins were calculated and are listed in Table 2. The theory predicts that the critical composition will be skewed toward the lower molecular weight component, which for these blends is the epoxy resin. Increasing the PPE molecular weight only increases the molecular weight disparity and further shifts the critical point toward higher epoxy compositions. Each critical composition blend was prepared and its phase separation temperature (T_{ps}) experimentally measured. These values are also recorded in Table 2. Additionally, the T_{ps} for Epon828 blends with unmodified PPE resins are plotted in Fig. 3 as open points that have been connected by a dashed lint to highlight the shift.

Although, a complete study of the miscibility of Epon825 with PPE resins was not performed, Fig. 4(a) compares the phase behavior of analogous blends of either Epon825 or Epon828 with 0.12 IV PPE. The blends with Epon825 show enhanced miscibility with a USCT phase boundary roughly 20 °C lower than that for the blends with Epon828. Fig. 1 shows that these epoxy resins share very similar molecular structures, but Epon828 has on average an additional bisphenol-A repeat unit as well as an aliphatic hydroxyl

Table 2
Blend critical compositions, phase separation temperatures, and calculated interaction energies

PPE Type	Epon825 $\phi_{\text{critical,PPE}}$	T_{ps} (°C)	B_{critical} (J/cm^3)	Epon828 $\phi_{\text{critical,PPE}}$	T_{ps} (°C)	B_{critical} (J/cm^3)
PPE.09	0.195	62	7.04	0.199	75	7.02
PPE.12	0.169	85	7.07	0.172	100	7.05
PPE.15	0.147	100	6.98	0.15	121	7.06
PPE.25	0.104	135	6.93	0.107	151	6.88
PPE.30	0.088	148	6.90	0.09	171	6.94
PPE.15FA4	0.143	115	7.21	0.147	131	7.18
PPE.15FA8	0.144	129	7.47	0.147	148	7.49
PPE.12MC	0.162	103	7.71	0.165	118	7.26

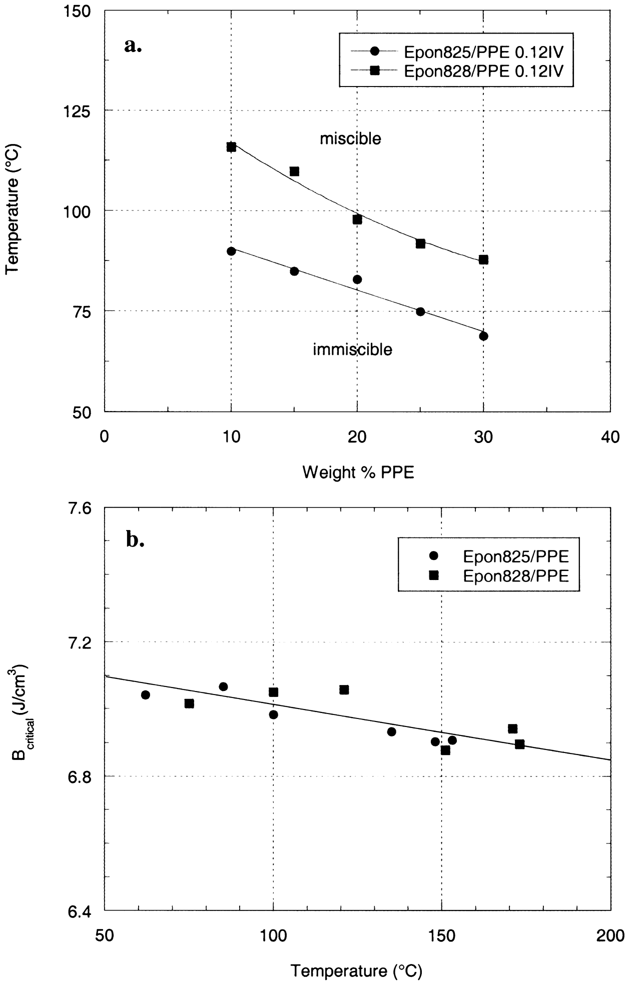

Fig. 4. (a) Phase behavior of 0.12 IV PPE blends with Epon825 and Epon828 demonstrating the effect of epoxy structure/molecular weight; curves indicate trends in the data only. (b) Critical interaction energy densities, B_{critical}, for epoxy and PPE molecular structures calculated using phase separation temperatures measured for the critical composition blends summarized in Table 2.

group. Mixing thermodynamics can be used to decipher how the differences in the epoxy structure and molecular weight influence the change in miscibility. For this analysis, critical composition blends of Epon825 with PPE were studied. By using the phase separation temperatures measured for critical composition blends, Eq. (2) was used to calculate estimates for the critical interaction energy. These results are listed in Table 2 and plotted in Fig. 4(b) for both Epon825 and 828. To a good approximation, it appears that one, slightly temperature dependent B_{critical} describes the interaction between PPE and either DGEBA epoxy. Thus, the difference in phase behavior in Fig. 4(a) arises from the difference in epoxy molecular weight. The additional hydroxyl group in Epon828 appears to have negligible effect on the interaction with the PPE resins.

Now that the interaction energy between DGEBA resins and PPE has been estimated, the Flory–Huggins theory can be used to predict the temperature dependent miscibility. To do so, a linear expression for B_{critical} was made with a least-squares fit to the data in Fig. 4(b). With this expression and Eq. (1), free energy of mixing curves were calculated and graphical evaluation of coexistence points used to estimate binodal phase boundaries. Additionally, spinodal phase boundaries were calculated directly by setting the second derivative of Eq. (1) with respect to composition equal to zero. The results of these predictions are shown in Fig. 5(a) for the PPE molecular weights studied experimentally. The actual phase behavior measurements for these blends at off-critical compositions can be best compared with the predictions of the binodal phase boundaries since the mobility of these systems is high, and rapid phase rehomogenization and separation was observed above and below the phase boundary. The observation that cloud point measurements were found to be invariant with cooling rate also supports this comparison. Fig. 5(b) shows an overlay of the data from Fig. 3 with the binodal predictions. As a consequence of this analysis technique, the data and predictions match quite well at the critical compositions. At off-critical compositions reasonable agreement is also found. Differences between predicated and experimental maximums in the phase boundary may arise from polydispersity effects as discussed earlier. The fact that the deviation is greatest with the lower molecular weight, more polydisperse PPE resins is consistent with this possibility.

At low PPE contents, less than 10 wt%, it is reasonable that the model predicts an increase in miscibility. Poor phase contrast at such loadings however, precludes experimental verification. Limitations of the Flory–Higgins theory and of some of the assumptions applied are nonetheless recognized. These include the non-specific treatment of strong interactions such as hydrogen bonding. A Painter–Coleman analysis can be used in attempts to explicitly quantify such interactions [21]. In this study, these effects were absorbed into the B interaction parameter. Furthermore, possible compositional dependence of the interaction parameter was neglected. Equation-of-state effects can also play an important role in phase behavior and accounting for these requires use of more advanced and necessarily complex theories. Even after acknowledging these limitations, the agreement shown in Fig. 5(b) with respect to molecular weight, temperature, and composition dependence is reasonably good and well serves the goals of this work.

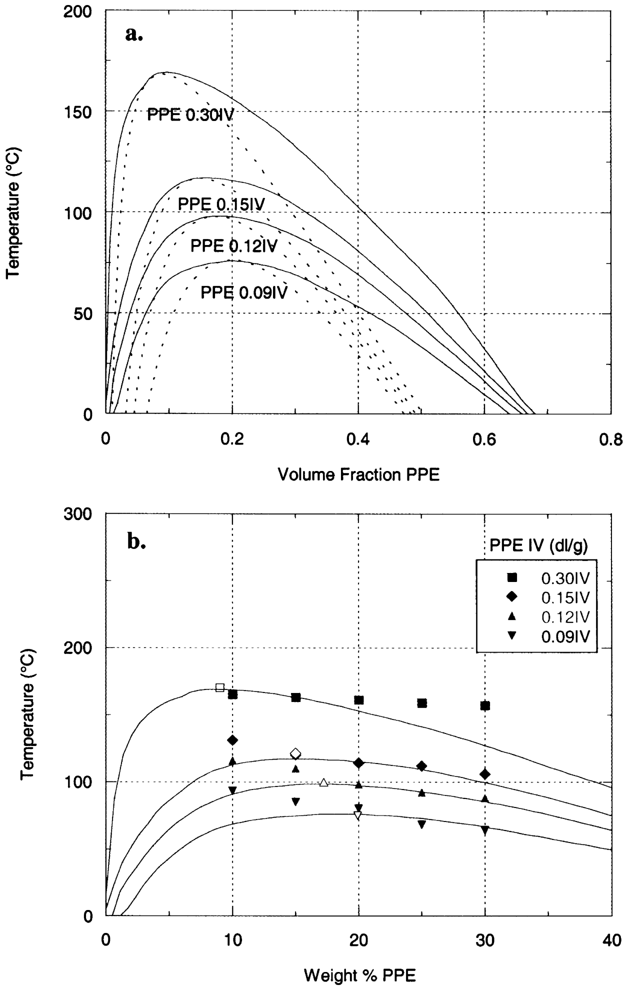

Fig. 5. (a) Binodal (solid line curves) and spinodal (dashed line curves) UCST phase boundaries calculated for PPE/Epon828 blends using the temperature dependent interaction energy density shown in Fig. 4(b) and the Flory–Huggins theory of mixing.(b) Overlay of calculated binodal phase boundaries with experimentally measured phase behavior from Fig. 3.

3.2. Miscibility of modified PPE resins

The PPE structure can be chemically altered in numerous ways to change its reactivity with the epoxy during cure. It is critical to know how these modifications affect the blend miscibility. Conversely, it may be desirable to tailor the PPE chemistry in ways to enhance miscibility without affecting reaction chemistry.

To determine whether PPE hydroxyl groups contribute the to miscibility with DGEBA, a methyl capped 0.12 IV PPE was studied. The methyl capping effectively eliminated all hydroxyl groups as confirmed by ^{1}H-NMR. Fig. 6(a) compares the phase behavior of Epon828 blends with unmodified and methyl capped PPE. Because GPC shows these PPE resins are nominally the same molecular weight, the reduction in miscibility observed upon capping can be attributed to interactions associated with the hydroxyl groups. Capping the hydroxyl groups might eliminate hydrogen bonding with the epoxy resin. The associated interactions energies were quantified by studying critical composition blends. Since only one molecular weight of capped PPE was made, only two critical composition blends, one with each of the two epoxy resins, could be studied. The B_{critical} values calculated for the two blends are plotted in Fig. 6(b) along with the unmodified PPE/DGEBA epoxy interaction energies replotted from Fig. 4(b). By this treatment of the energetics, it is clear that methyl capping makes the interaction measurably more endothermic, i.e. more unfavorable for mixing.

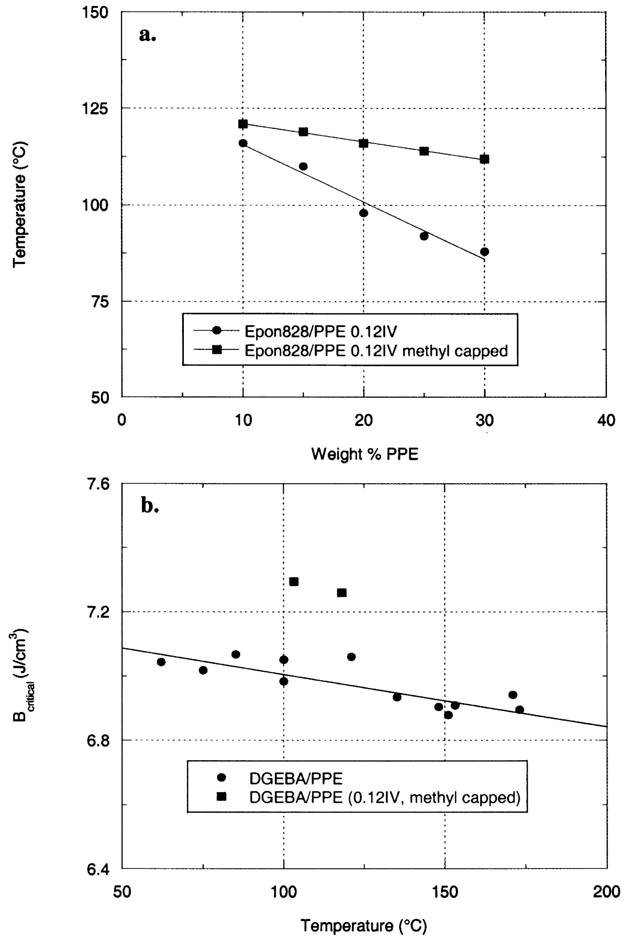

Fig. 6. (a) Methyl capping of PPE hydroxyl groups causes a decrease in miscibility with Epon828 epoxy resins. (b) The change can be attributed to a more endothermic critical interaction energy as shown in comparison to the DGEBA/PPE interaction energies from Fig. 4(b).

Many methods for adding acid functionalities to PPE exist but one of the simplest is to reactive extrude the thermoplastic with an organic acid. This was performed with two levels of FA to produce the FA modified 0.15 IV PPE resins described in Table 1. The miscibility of the resins with Epon828 is compared to the unmodified resin in Fig. 7(a), while the corresponding interactions calculated from critical compositions are plotted in Fig. 7(b). Like methyl capping, acid modification reduces miscibility, increasingly so with acid level, and can be quantified in terms of increasingly endothermic interaction energies. In this case, it is possible that specific interactions and/or reactions involving the acid-derived chemistries may be important. Not only could have the modification eliminated favorable hydroxyl interactions with the epoxies but it may also have added moieties that preferably self-associate within the PPE phase.

It is also conceivable that the acid moieties on the PPE chains or unreacted FA trapped in the PPE resin may have

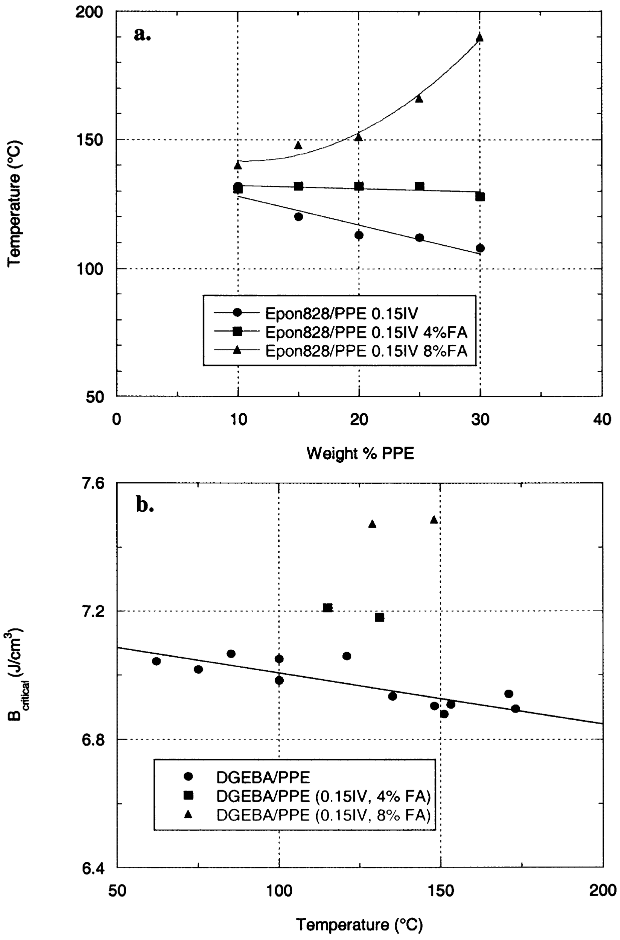

Fig. 7. (a) Effect of grafted acid functionality on the phase behavior of PPE with Epon828 epoxy resin. Increasing grafting level decreases the miscibility as evidenced by the shift of the UCST phase boundary to higher temperatures. (b) B_{critical} values calculated using the phase behavior of critical composition blends with both Epon825 and Epon828. For comparison, the B_{critical} values from Fig. 4(b) for non-grafted PPE are included in the plot.

reacted with the epoxy. Since phase separation was observed upon cooling these blends and was reversible, only limited formation of covalent linkages between PPE and epoxy seems likely. If acid-catalyzed reaction of epoxy groups caused the epoxy molecular weight to build, the decrease in miscibility observed could be due to the resulting decrease in the combinatorial entropy of mixing. It would be difficult to see this change with GPC but a controlled NMR or IR study might be used to probe this chemistry. The possibility of these reactions is considered further within the context of gelation during the cure and in the final blend morphology.

3.3. Phase separation and gelation during reaction

Up to this point, all experiments have been conducted on non-reacting systems. It is now interesting to investigate how these findings play out in analogous systems that undergo cross-linking reactions. To this end, the effects of PPE molecular weight, loading, and functionality on the reaction time to reach phase separation and gelation were investigated. These results are shown in Fig. 8 Phase separation and gelation measurements, connected using dashed and solid line curves, respectively, were made during the curing reaction of Epon828/PPE blends at 150 °C using MDEA curing agent. Replicate blends were measured to obtain the estimates for error indicated in the plot. Blends with the 8% FA-grafted PPE were not included in this study because of their limited miscibility at 150 °C.

The potential reaction between epoxy and PPE hydroxyl groups is believed to be relatively insignificant for the systems under investigation as supported by studies in the literature [22]. This simplifies the thermodynamic treatment of phase separation in blends with unmodified PPE as the point where combinatorial entropy of mixing no longer favors miscibility owing to the increase in epoxy molecular weight with network formation. Thus, a more miscible PPE/epoxy blend will not phase separate until a higher extent of reaction. In this context, the measurements of phase separation during isothermal reaction given in Fig. 8 are consistent with miscibility measurements shown previously in Fig. 3 Lowering PPE molecular weight or increasing its content in the blend enhances miscibility and causes an increase in the time to phase separation during reaction. In contrast, with the 4% FA-grafted PPE variant, miscibility is decreased relative to blends containing unmodified PPE, particularly at higher loadings as shown if Fig. 7(a), and earlier phase separation times are observed. Other factors may contribute to the reduced time to phase separation. Faster molecular weight build with the incorporation of the acid-grafted PPE into the network may play a role but at the same time copolymer formation could have a compatibilizing effect. The presence of acid could also be catalyzing a faster cross-linking reaction.

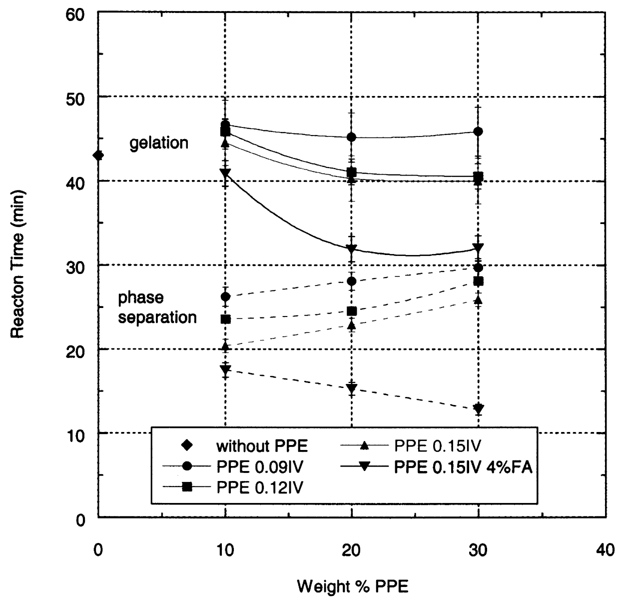

Fig. 8. Reaction time to phase separation (dashed lines) and gelation (solid lines) measured during the curing reaction of Epon828/PPE blends at 150 °C using MDEA curing agent.

Fig. 8 shows that a neat epoxy gels after 43 min (standard deviation of 0.5 min. based on five replicates). The overall effect of adding up to 30 wt% unmodified PPE is minimal and, accounting for large measurement standard deviations of up to 2.5 min, possibly insignificant. An appreciable reduction in gel time of more than 10 min is recorded when 20 and 30 wt% of the 4% FA-grafted PPE is blended with the epoxy.

This might be attributed to earlier formation of an infinite network, arrested reaction due to vitrification (i.e. encroachment of the building network glass transition on the cure temperature), and/or faster reaction kinetics. The first effect can be checked by considering that the acid-grafted PPE contains on average only 1.4 functionalities per chain [8] whereas a functionality of greater than 2 is required to act as an effective cross-linker. Simple Carothers type calculations based on the degree and amounts of chemical effect on the reaction conversion required to achieve gelation [23]. In fact, if the PPE were to remain miscible in the epoxy matrix phase it may actually reduce the cross-link density.

There is a strong possibility that grafted acid moieties in the PPE have a catalytic effect on the curing reaction. It is known that organic acids and cyclic anhydrides, both expected derivatives in the acid grafting reaction, can react with epoxy groups by addition esterification particularly in the presence of a base such as the MDEA curing agent [24]. Isothermal DSC experiments at 150 °C for 2 h were performed to investigate three formulations: Epon828/MDEA control, control plus 20 wt% PPE.15, and control plus 20 wt% PPE.15FA4. The results from these tests are summarized in Table 3 along with gel time results extracted from Fig. 8 for comparison.

From isothermal studies the time to peak exotherm was obtained. Also, because statistical calculations predict that

Table 3
DSC thermal analysis of selected systems

	Control: Epon828/MDEA	Control + 20 wt% PPE.15	Control + 20 wt% PPE.15FA4
DSC Isothermal at 150 °C			
Exotherm Peak (min)	27	31	22
ΔH_{rxn} (J/g)	−284	−259	−257
Time (min) to 58% cure at 150 °C	39	39	32
Conversion (%) at measure gel point	66	60	57
$T_g(s)$ (°C) after isothermal	120	121/154	121/155
$T_g(s)$ (°C) after follow-up scan to 275 °C	141	139/181	139/177
Gel Point (from Fig. 8)			
Time to Gel at 150 °C (min)	43	40	32

this system will gel after 58% reaction conversion [23], the time to achieve this level of cure was also estimated from the DSC results. These values are included in Table 3 along with the DSC conversion that corresponds to the actual gel time measurements. In general, the gel time and DSC results are in good agreement and suggest that PPE.15 has little impact on the reaction rate whereas the acid-grafter PPE speeds the reaction and reduces the gel time by 10 min. Quantitatively, the predicted gelation at 58% conversion slightly underestimates measurements made in the control and the PPE.15 modified systems but it is right in line for the acid-grafted PPE blend. This prediction is known to provide conservatively low estimates because it assumes equal and complete functional group reactivity. Heat of reaction estimates are included in Table 3, and for blends containing 20 wt% PPE these have been corrected to account for the effective dilution of reactive components. Even after this correction, incorporation of PPE, unmodified or acid-grafted, lowers the measured reaction exotherm by approximately 10 percent. Follow-up DSC temperature scans to 275 °C at 10 °C/min capture no residual heat of reaction but do suggest additional reaction in all the systems as evidenced by upward shifts in the cured glass transition temperatures. These glass transition values are recorded in Table 3. Additional details on the DSC evaluation of PPE modified epoxy systems have been published elsewhere [8]. Overall, the combined gel time and DSC results help to show that the unmodified PPE has little effect on the epoxy reference system whereas the acid-grafted PPE increases the reaction rate as well as reduces the conversion required to reach the gel point.

To probe the effect of temperature on the curing reaction and phase behavior, Epon828 was cured with and without 20 wt% PPE.12 at temperatures between 150 and 200 °C with the results shown in Fig. 9. At temperatures greater than 150 °C, addition of PPE may appear to slightly increase the gel time relative to the unfilled blend but given the error of the measurement the difference is not statistically significant. In the blends containing PPE, time to phase separation was concurrently studied as a function of temperature. These measurements are including in Fig. 9. Since phase separation is believed to be caused by epoxy molecular weight climbing to a threshold value during reaction and gelation is similarly linked to the epoxy molecular weight, these two responses would be expected to have a similar temperature dependence if mass transfer of phase separation is fast compared to the rate of reaction. However, the window of time between phase separation and gelation narrows in Fig. 9 as the cure temperature is increased. Phase separation appears to be less responsive to temperature. This suggests increasingly mass transfer limited phase separation may be born out at higher temperatures. This will be considered further in terms of the final blend morphology.

3.4. Morphology

The preceding miscibility studies have demonstrated that these systems are initially homogeneous but phase separate during cure. Fig. 10 depicts schematically how morphology begins to develop at the reaction conversion where phase separation begins and may continue to develop and coarsen up to the reaction conversion where the gel point is reached. It has been shown that post cure annealing can induce a

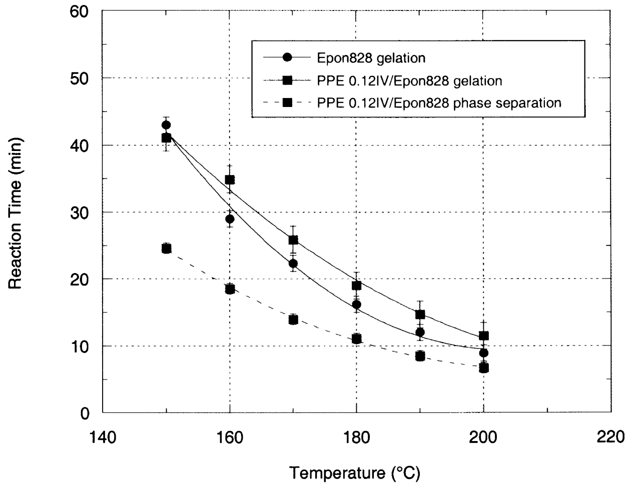

Fig. 9. Effect of curing temperature on Epon282 gelation time (solid lines curves) with and without 20 wt% 0.12 IV PPE, and the concurrent phase separation in blends with PPE (dashed line curve).

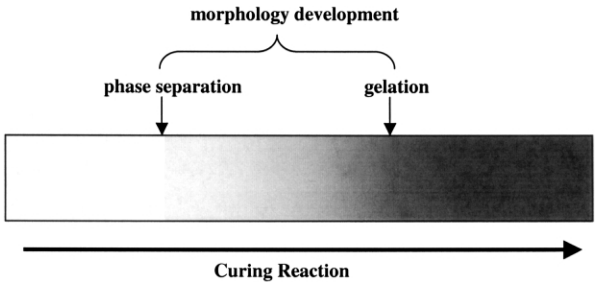

Fig. 10. Schematic of curing reaction identifying the window between phase separation and gelation, within which morphology can develop. Phase separation is driven by mixture thermodynamics while gelation is dictated by reactant functionality and stoichiometry. Control of these two points and the kinetics of the curing reaction may allow optimization of the cured blend morphology, and hence, physical (mechanical, electrical, chemical) properties.

change in the original annealed morphology but only when performed at temperatures above the original cure temperature and above the glass transitions of the materials involved [25]. The thermodynamics of mixing dictate phase separation while chemical functionality and reactive group stoichiometry strongly influence the extent of reaction at gelation. Control of PPE molecular weight and functionalization affords an opportunity to affect both of these points as shown in Fig. 8, and temperature may be used to alter the relative kinetics of phase separation and reaction as suggested in Fig. 9. How this impacts the cured morphology is now considered.

The effect of PPE content on PPE/epoxy morphology is demonstrated in Fig. 11 for Epon828 blends with 10, 20, and 30 wt% 0.12 IV PPE cured at 150 °C. The average dispersed PPE phase size was estimated to be, correspondingly, 1.5, 1.7, and 2.0 μm by image analysis. If morphology development was limited by mass transfer, the opposite trend might be expected because blend viscosity increases by an order of magnitude in going from 10 to 30 wt% 0.12 IV PPE at 150 °C [8]. Furthermore, the results in Fig. 8 suggest that the time available for phase development to occur may actually get smaller at higher PPE compositions. Since mass transfer does not appear to be limiting, this trend of increasing domain size with PPE content may simply reflect the volume fraction dependent probability that sites of phase separating PPE may overlap and coalesce into larger domains. Image analysis of the micrographs in Fig. 11 shows that the volume fraction of the dispersed phase closely corresponds to the PPE composition in the blend. Dynamic mechanical analysis (DMA) of analogous systems reported elsewhere [8] showed minimal shifting of the loss peaks in the phase separated materials from their neat components. This combined TEM and DMA data as well as the glass transition data included in Table 3 suggest nearly complete component segregation in the separated phases.

Fig. 12 shows that with a constant PPE composition of 20 wt%, increasing PPE molecular weight likewise increases the size of the phase dispersed within the Epon828 matrix. The average dispersed phase size was estimated to be 1.4, 1.7, and 1.9 μm for the 0.09, 0.12, and 0.15 IV PPE resins. Again, this trend cannot be explained in terms mobility effects because blend viscosity actually increases by a factor of two in going from a blend with 20 wt% 0.12 IV PPE to a blend with the same amount of a 0.15 IV PPE [8]. Referring back to Fig. 8, the window of time for morphology development shrinks slightly as PPE molecular weight is lowered due to the upward shift in the phase separation time (assuming negligible change in the gel point). If this causes gelation to occur before coalescence is complete, blends with lower IV PPE may be expected to have more finely dispersed domain sizes trapped in the morphology. The possibility that the thermodynamic effects such as a change in interfacial energy with PPE molecular weight may also contribute to these results. To verify that the PPE hydroxyl end groups do not play such a role it would have been interesting to compare these results with corresponding blends made with a methyl capped PPE resin. However, because of limited methyl capped material this could not be studied here.

Use of an acid-grafted PPE complicates the story as discussed earlier owing to possible compatibilization reaction, catalyzed reaction rate, and altered phase behavior,

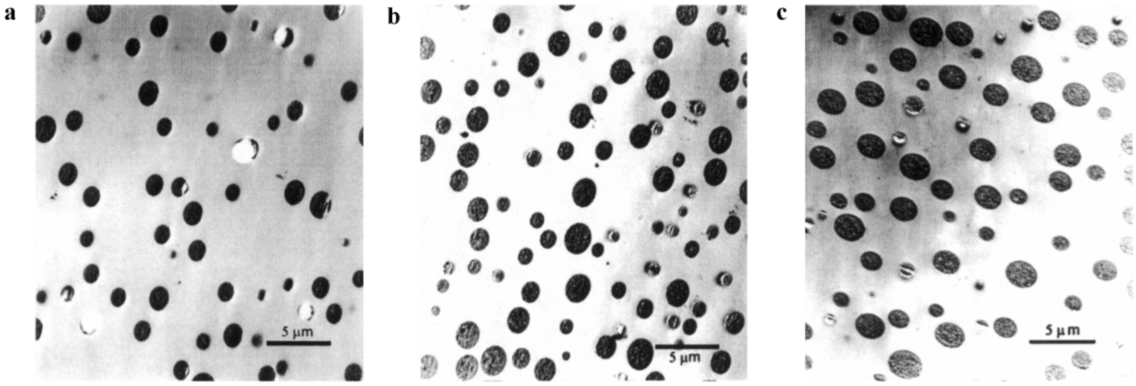

Fig. 11. Increasing the content of 0. 12 IV PPE in a cured blend with Epon828 from 10, to 20, to 30 wt%, corresponding to micrographs a, b, and c, increases the average size of the dispersed PPE phase morphology from 1.5, to 1.7, to 2.0 μm.

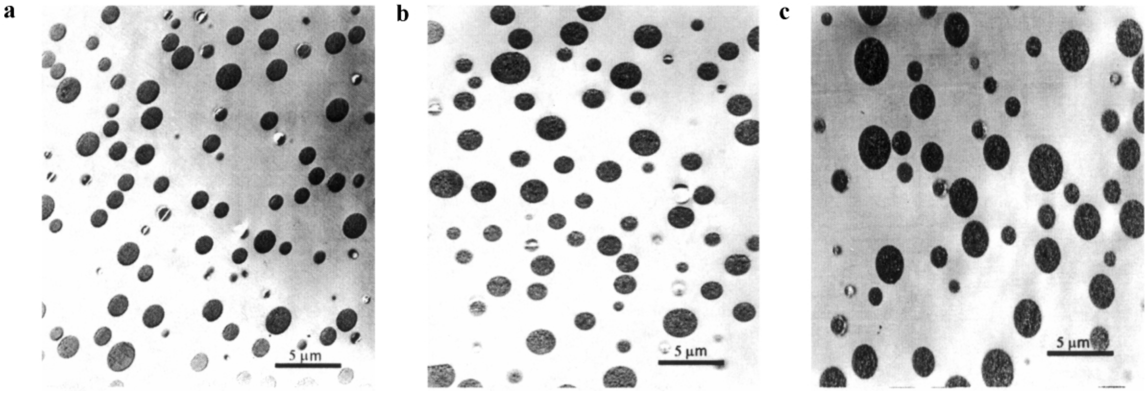

Fig. 12. Cured blends of Epon828 with 20 wt% 0.09, 0.12, and 0.15 IV PPE corresponding to micrographs a through c, with average dispersed phase sizes of 1.4, 1.7, and 1.9 μm, respectively.

and gives rise to some interesting effects in the cured morphology. Fig. 13 summarizes this for blends containing 10, 20, and 30 wt% of the 4% FA-grafted PPE. Dispersed PPE-rich phases were measured to be 1.3 and 1.5 μm for the blends containing 10 and 20 wt% PPE, respectively, while addition of 30 wt% caused regions of phase inversion to form. Comparison of the micrograph in Fig. 13(b) with its non-grafted analogue in Fig. 12(c) shows that the acid functionality acts to decrease the PPE phase size from 1.9 to 1.5 μm. Therefore, even though acid grafting was shown to decrease PPE miscibility in Fig. 7 and reduce the reaction time to phase separation in Fig. 8, the resulting morphology suggests that the acid groups may be reacting into the epoxy matrix and preventing complete phase separation or coalescence. The increased level of functionality gives a more compatibilized morphology. The inversion of the phase in Fig. 13(c) is possibly the result of a multistage process of phase separation where separation first occurs between an epoxy rich and PPE-rich phase, and then upon further reaction, each of these again phase separate. Although, outside the scope of this investigation, DMA analysis would be a useful method to more closely probe the final compositions of the phase separated morphologies while temperature modulated DSC would be a powerful means of studying this interesting phase behavior in situ as demonstrated in the literature [3]. Detailed electrical, mechanical, and thermal evaluations on some of the cured systems investigated here can be found elsewhere [8].

Finally, it is interesting to explore how cure temperature influences the cured morphology. The morphologies of Epon828 blends with 20 wt% 0.12 IV PPE cured at temperatures of 150, 175, 200 °C are summarized in Fig. 14(a)–(c) with corresponding dispersed phase dimensions of 1.7, 2.0, and 1.3 μm, respectively. Although the window of time between phase separation and gelation collapses for these materials at higher temperatures as shown in Fig. 9, comparison of micrographs a and b shows an increase in disperse PPE phase size from 1.7 to 2.0 μm. Since Fig. 6(b) suggests the thermodynamic interaction does not change significantly over this temperature range, the difference may be a result of increased mobility at higher temperatures that allows the PPE-rich phase to coalesce. Micrograph c demonstrates that it is possible to increase the reaction kinetics relative to phase separation kinetics with temperature to a point where gelation occurs before complete phase coalescence. The existence of a maximum in the size of the

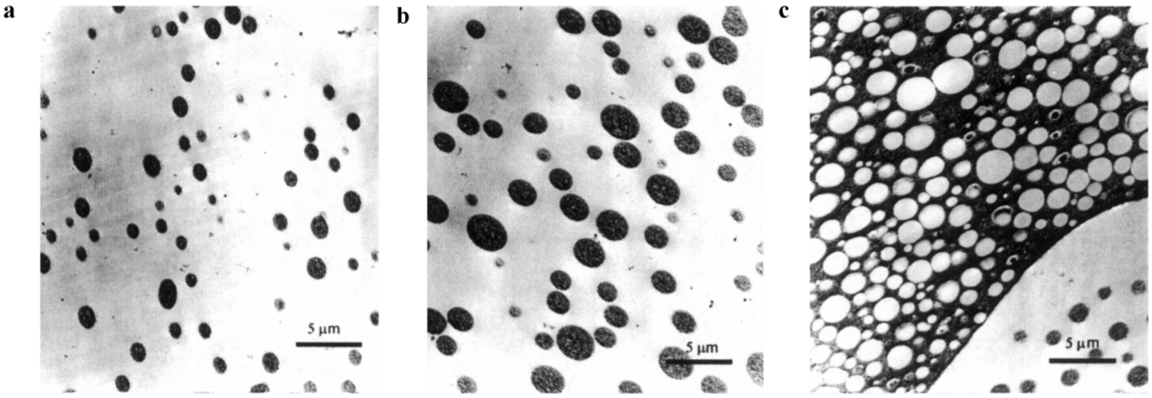

Fig. 13. Cured morphology of blends of Epon828 with 10, 20, and 30 wt% 0.15 IV PPE grafted with 0.45 mequiv. of acid functionality per gram of PPE. At 10 and 20 wt% compositions, the PPE is the dispersed phase with average diameters of 1.3 and 1.5 μm, respectively, whereas at 30% wt%, regions of phase inversion are observed.

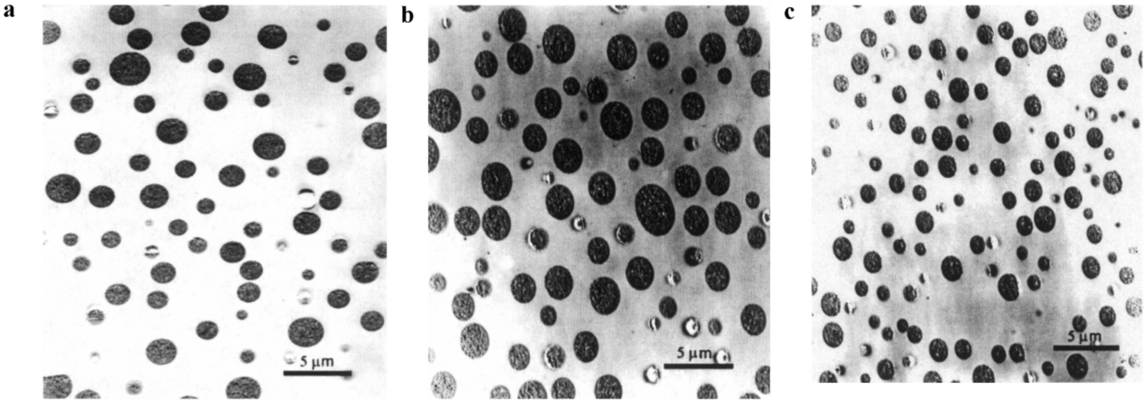

Fig. 14. Blends containing 20 wt% 0.12 IV PPE in Epon828 cured at temperatures of 150, 175 and 200 °C, corresponding to morphologies in micrographs a, b, and c with disperse phase sizes of 1.7, 2.0, and 1.3 µm, respectively.

dispersed phase as a function of temperature has been predicted in theoretical models reported in the literature [14].

4. Conclusions

The miscibility of DGEBA with a series of PPE resins was measured and then interpreted with the Flory–Huggins theory. Both methyl capping and acid grafting of PPE were found to reduce the miscibility with the epoxy resins because of more endothermic interactions, while lower PPE molecular weight improved miscibility owing to the larger entropic contribution to the free energy of mixing. Trends of greater miscibility in the non-reacted blends translate to the reacting systems as phase separation being shifted to later stages of the curing reaction. These observations are consistent with phase separation occurring due to the increase of epoxy molecular weight during cross-linking. Addition of unmodified PPE, regardless of molecular weight or content, had minimal affect on the measured gel point beyond what might be inferred as viscosity effects. In contrast, blends with acid-grafted PPE gelled considerably more rapidly, predominantly due to a faster reaction rate in the presence of the acid moieties but also in part because of reaction of the PPE into the cross-linked network. Evidence of the latter was observed in the morphology of blends containing acid-grafted PPE that showed suppression of coalescence compared to the non-modified PPE resin. Morphology studies also revealed trends of increasing dispersed phase size with either PPE content or molecular weight. To a limit, increasing reaction temperature was shown to produce an increase in the dispersed phase size, most likely due to an increase in molecular mobility. Then at higher temperatures, a smaller dispersed phase size was trapped into the morphology, possibly due to an increase in the rate of reaction relative to phase separation. This work has demonstrated how the cured morphology can be influenced with control of PPE molecular weight, content, and functionality as well as with reaction temperature. This allows the opportunity to create materials with tailored properties.

Acknowledgements

The authors would like to gratefully thank Stan Hobbs, Mike Takemori, and Vicki Watkins for many helpful discussions and the use of microscopic equipment, and Chin Lee for his TEM characterization of the cured morphologies.

References

[1] Pascault JP, Williams RJJ. Formulation and characterization of thermoset-thermoplastic blends. In: Paul DR, Bucknall CB, editors. Polymer blends, vol. 1: formulation. New York: Wiley; 2000. p. 379–415.
[2] Bucknall CB, Gomez CM, Quintard I. Polymer 1994;35(2):353–9.
[3] Swier S, Van Mele B. Thermochimica Acta 1999;330:175–87.
[4] Gomez CM, Buckenall CB. Polymer 1993;34(10):2111–7.
[5] Chen J, Chang F. Macromolecules 1999;32(16):5348–56.
[6] Pearson RA, Yee AF. J Appl Poly Sci 1993;48(6):1051–60.
[7] Pearson RA, Yee AF. Polymer 1993;34(17):3658–70.
[8] Yeager GW, Anostario JM, Merfeld GD, Takemori MT, Hutchins GA. The use of low molecular poly(phenylene ether) resin in epoxy thermosets, SAMPE Annual Conference, Long Beach, CA; 1999.
[9] Ishii Y, Ryan AJ. Macromolecules 2000;33(1):158–66.
[10] Jansen BJP, Meijer HEM, Lemstra PJ. Polymer 1999;40:2917–27.
[11] Bucknall CB, Davies P, Partridge IK. Polymer 1985;26:109–12.
[12] Bucknall CB, Partridge IK, Phillips MJ. Polymer 1991;32(5):786–90.
[13] Wu HD, Chu PP, Ma CCM, Chang FC. Macromolecules 1999;32(9): 3097–105.
[14] Williams RJJ, Borrajo J, Adabbo HE, Rojas AJ. A model for phase separation during a thermoset polymerization. In: Reiw CK, Gillham JK, editors. Advances in chemistry series, vol. 208. Washington, DC: American Chemical Society; 1984. p. 195.
[15] Vazquez A, Rojas AJ, Adabbo HE, Borrajo J, Williams RJJ. Polymer 1987;28:1156–64.
[16] Flory PJ. J Chem Phys 1942;10:51.
[17] Huggins ML. J Chem Phys 1941;9:440.
[18] Koningsveld R, Chermin HAG. Proc R Soc London, A 1970;319:331.

[19] Koningsveld R, Kleinntjens LA. J Polym Sci, Polym Symp 1977;61:221.

[20] Sollich P. J Phys: Condens Matter 2002;14(3):R79–R117.

[21] Coleman MM, Graf JF, Painter PC. Specific interactions and the miscibility of polymer blends. Lancaster, PA: Technomic; 1991.

[22] Riccardi CC, Williams RJ. J Appl Polym Sci 1986;32(2):3445–56.

[23] Odian G. Principles of polymerization, 2nd ed. New York: Wiley; 1970.

[24] Lee H, Neville K. Epoxy-resin curing mechanisms. Handbook of epoxy resins, New York: McGraw Hill; 1982.

[25] Girard-Reydet E, Vicard V, Pascault JP, Sautereau H. J Appl Polym Sci 1997;65(12):2433–45.